ELSEVIER

Biochimica et Biophysica Acta 1191 (1994) 164–172

BBA Biochimica et Biophysica Acta

Thermodynamics of transfer of indocarbocyanines from gel to fluid phases of phospholipid bilayers

Charles H. Spink *, Debbie Clouser, John O'Neil

Chemistry Department, State University of New York-Cortland, P.O. Box 2000, Cortland, NY 13045, USA

(Received 26 August 1993)

Abstract

Application of the regular solution model to thermal transition data obtained by differential scanning calorimetry has allowed the determination of partition coefficients, K_p, and the thermodynamics of transfer of a series of indocarbocyanine solutes between the gel and fluid phases of phospholipid bilayers. The indocarbocyanines with alkyl chain lengths of 12 to 22 carbons were partitioned between dipalmitoyl- and distearoylphosphatidylcholine phases at the transition temperatures of the gel–liquid-crystal phase transition. The results indicate that as the alkyl chain length of the solute nears that of the acyl chains of the bilayer lipid, the free energy of transfer from gel to fluid is least negative, and the enthalpy of transfer is most positive. There is almost complete entropy-enthalpy compensation in the transfer process. Comparison of the partition coefficients with published values determined by a fluorescence method show good agreement when the differences in temperature of the measurements are accounted for.

Key words: Scanning calorimetry; Bilayer; Indocarbocyanine; Partitioning; Phospholipid; Thermodynamics; Regular solution

1. Introduction

The partitioning of membrane-soluble molecules between gel and fluid-phase lipid has been studied in order to understand better the interactions between bilayer lipids and membrane components [1–10]. Solute properties, such as diffusion and a variety of spectral transition characteristics, are known to be affected by whether the solute is dissolved in fluid or gel-phase lipid [2–9]. On the other hand, the properties of bilayer membrane lipids often show remarkable sensitivity to the presence of solutes in the bilayer [11,12,15]. For example, solutes which partition strongly into the fluid phase of thermally-active lipids depress the gel-fluid transition temperature, while those solutes which prefer the gel-phase environment increase the transition temperature [11]. Thus, there are specific interrelationships between the structure and the energetics of the lipid-solute interactions that determine the nature of solute behavior in biological membranes. Partitioning data can provide a framework for understanding lipid bilayer interactions, since the partition coefficient magnitude responds to the structural features of the solute and bilayer lipid, and to the energetics of the mutual interactions involved [6–9,18].

Differential scanning calorimetry (DSC) is a sensitive tool for the study of gel-fluid phase equilibria [12,14,15]. The phase transition temperature is altered in the presence of solutes, and has been used to evaluate partition coefficients of bilayer solutes between gel and fluid phase [12,15,19]. A limitation of the method for the study of solute–lipid interactions in the bilayer is that the data analysis requires certain as-

* Corresponding author. Fax: +1 (607) 7535999.

Abbreviations: C_nDiI, 1,1'-dialkyl-3,3,3',3'-tetramethylindocarbocyaneperchlorate, where n is the number of carbon atoms in the alkyl chain; DPPC, 1,2-dipalmitoyl-*sn*-glycero-3-phosphocholine; DSPC, 1,2-distearoyl-*sn*-glycero-3-phosphocholine; (7,6) PC, 1-acyl-2-[2-(6-carboxyhexyl)-2-octyl-4,4-dimethyloxazolidinyl-3-oxy]-*sn*-glycero-3-phosphocholine.

SSDI 0005-2736(93)E0375-K

sumptions about the nature of the lipid-solute solutions both in gel and fluid phase. Examination of phase diagrams of typical phospholipid mixtures reveals evidence of nonideal mixing of the components in both gel and fluid phase [20–22]. Thus, to evaluate partition coefficients assuming that ideal solutions are formed seems inappropriate for most lipid-solute mixtures. This problem was pointed out by Ethier et al. [14], who studied in a qualitative way the effects of solute partitioning on the DSC transitions of thermally active lipids.

Recently, however, regular solution models have been used successfully both to predict phase diagrams and to determine solute effects on the transition temperatures of phospholipids mixed with a variety of solutes [19,22]. Agreement between experimental and predicted behavior has been quite good. In the regular solution model it is assumed that the entropy of mixing of solute with lipid in the bilayer is ideal in both fluid and gel phase, a condition which is often true in dilute solutions [19]. The nonideality is presumed to arise from an enthalpic contribution to mixing in both phases. Using this regular solution treatment it is possible to derive equations for the effects of partitioning solutes on the phase transition temperature.

We recently reported direct measurements of the partition coefficients of a series of indocarbocyanine dyes, C_nDiI, between various gel phases and a fluid, spin-labelled lipid, based on a fluorescence quenching technique developed by Feigenson and coworkers [4,6–9,18]. The partition coefficients showed a wide range of values, which depended on the relative lengths of the alkyl chains in the probe molecule and the length of the acyl chain of the lipid. The strongest partitioning into gel phase occurs when there is an approximate match of the alkyl chain lengths in the dye with those of the phospholipid.

Since the above partitioning data are available for the indocarbocyanines, and since there is precedent for using the regular solution model for evaluating the effects of solutes on the phase transition temperatures of thermally active phospholipids, this study presents a method for obtaining the partition coefficient between gel and fluid phase lipid from DSC data using the regular solution model, and the method is applied to the partitioning of the C_nDiI probes in mixtures with dipalmitoylphosphatidylcholine (DPPC) and distearoylphosphatidylcholine (DSPC). The partitioning results obtained by DSC are compared with the data from the fluorescence quenching technique described above. In addition, from the DSC measurements the enthalpy of transfer of the solutes between gel and fluid phase lipid can be determined. Thus, the free energy, enthalpy and entropy of transfer of the C_nDiI solutes can be evaluated from DSC data. Comparisons between data obtained assuming an ideal solution model with those of the regular solution approach are discussed.

2. Experimental

Materials. The DPPC and DSPC were obtained from Avanti Polar Lipids, Alabastar, AL, and the C_nDiI solutes purchased from Molecular Probes, Eugene, OR, and were used as received. Buffers were made up to 0.15 M NaCl, 0.02 M Na_2HPO_4, and the pH adjusted to 7.4 with concentrated HCl. Chloroform was Spectroquality, and the buffer components were Reagent Grade.

Preparation of vesicles. Multilamellar vesicles of DPPC or DSPC containing specified mole fractions of C_nDiI probes were prepared by mixing $CHCl_3$ stock solutions of lipid and solute at the appropriate ratio, evaporating the organic solvent under Ar, and removing the last traces of solvent by evacuating overnight. The proper amount of buffer was added to the dried lipid film so that the final concentrations of lipid were in the range of 0.10 to 0.50 mM. The samples were constituted by heating above the phospholipid phase transition temperature for 15 min, and then vortexing for about 25 s. This process was repeated at least two more times to insure that the lipid film was dispersed.

DSC measurements. Calorimetric measurements were made with a MicroCal MC-2 scanning calorimeter at a scan rate of 0.19 deg./min. Scans were repeated several times in order to assure that reproducible DSC traces were obtained, and the solute was properly equilibrated in the lipid mixtures.

Data analysis. According to the regular solution model developed by Inoue et al. [19], the transition temperature for the gel-liquid crystal phase transition of the lipid is related to mole fraction, X_s, of lipid soluble solute by the equation:

$$T_m = T_o + \frac{T_o}{H_o}\left(\Delta G_s^o\left[\frac{X_s}{1-X_s}\right] + \Delta U_s X_s\right) \quad (1)$$

where T_m is the temperature of half-melting of the gel-phase lipid, T_o is the transition temperature in the absence of solute, H_o is the calorimetric enthalpy of the lipid phase transition, ΔG_s^o is the standard free energy difference of the solute in the gel and fluid phases of lipid at T_o, and ΔU_s is the excess interaction energy (difference in excess enthalpy of the solute between fluid and gel phase), which determines the nonideality of mixing in the two phases. This equation is valid at low mole fraction as long as the entropy of transfer of the solute from gel to fluid phase lipid is concentration independent in the range of compositions studied. Inoue has shown this to be true for a number of solutes which partition between gel and fluid phase DPPC [19].

The limiting slope of a plot of T_m vs. X_s is:

$$\left(\frac{dT_m}{dX_s}\right)_{lim} = \frac{T_o}{H_o}[\Delta G_s^o + \Delta U_s] \quad (2)$$

since the term $X_s/(1-X_s)$ approaches X_s as $X_s \rightarrow 0$. From knowledge of T_o and H_o one can thus calculate $(\Delta G_s^o + \Delta U_s)$, which is the free energy of transfer of solute from gel to fluid phase, ΔG_{tr}, in dilute solution. Akin to Henry's Law behavior, if the excess free energy term in each phase can be considered constant in this dilute solution region, then the standard state for the dilute solution in each phase can be defined as that solution which results from extrapolation of the dilute region to unit mole fraction. The standard state in the gel phase will thus be a modified $P_{\beta'}$ phase, and the fluid phase will be akin to the L_α phase of DPPC. With that definition of the standard state, the value of ΔG_{tr} is related to K_p, the gel to fluid partition coefficient:

$$\Delta G_{tr} = [\Delta G_s^o + \Delta U_s] = -RT \cdot \ln(K_p) \quad (3)$$

If data are obtained over a wide enough range of mole fractions, such that nonlinearity occurs in the T_m vs. X_s plot, it is possible to use regression analysis to obtain independent estimates of ΔG_s^o and ΔU_s. However, in several of the cases with C_nDiI probes, when the mole fraction of solute is greater than about 0.05, a second thermal transition appears in the DSC scans, indicating that new phases of lipid are present. Because of this complication, DSC experiments were limited to compositions less than 5 mole percent C_nDiI. Under these circumstances the regression analysis leads to the limiting slope as defined above, and provides a direct method for obtaining the standard free energy difference of the solute between the two phases. Thus, we can evaluate ΔG_{tr}, and also obtain K_p from the free energies.

To evaluate T_m from the DSC experiments, it is necessary to calculate the area of the gel–fluid transition curve, and then to determine the point at which the fraction melted is 0.5. A computer program was written to perform this determination because T_m of the DSC transition curve does not necessarily correspond to the maximum in the excess heat capacity function for solute-broadened peaks. Then, from T_m vs. X_s plots the limiting slopes are evaluated and multiplied by the ratio, (H_o/T_o), in order to obtain the values of ΔG_{tr}. The melting points of the pure lipids were found to be 41.4 ± 0.05 and 54.1 ± 0.05°C from the intercepts of the T_m vs. X_s plots, for DPPC and DSPC, respectively. These values agree very well with the T_o values obtained on samples of the pure lipids.

The enthalpy change for the gel-fluid phase transition of pure DPPC was found to be 8.5 ± 0.5 kcal/mol, and for pure DSPC, 10.3 ± 0.8 kcal/mol. The calorimetric enthalpies were found to vary slightly with increasing mole fraction of solute, which is confirmation that the mixtures are showing nonideality in one or both lipid phases. One can evaluate the enthalpy of transfer of the solute from gel to fluid phase by Eq. (4):

$$\Delta H_c = \Delta H_o + \left(\frac{X_s}{1-X_s}\right) \cdot \Delta H_{tr} \quad (4)$$

Here ΔH_c is the calorimetric enthalpy per mole of thermally active lipid in the presence of solute at mole fraction X_s, ΔH_o is the enthalpy in the absence of solute, and ΔH_{tr} is the enthalpy of transfer of solute from gel to fluid lipid [15]. Thus, a plot of ΔH_c vs. $(X_s/(1-X_s))$ has a slope of ΔH_{tr}, and since ΔG_{tr} is obtained from the T_m vs. X_s fitting, it is possible to evaluate the entropy of transfer of solute, ΔS_{tr}, from gel to fluid phase lipid.

3. Results

DSPC-C_nDiI data

Fig. 1 shows representative DSC transition curves for several compositions of C_nDiI in DSPC. In most cases there is a depression of the melting temperature, and a concommittent broadening of the transition curve with increased concentration of the solute. Also, the excess heat capacity maximum, $C_{p(m)}$, decreases in all cases as the concentration of C_nDiI increases in the mixtures. Note that the transition curves for the C_{20}DiI show only a slight T_m lowering and relatively little broadening, although $C_{p(m)}$ does decrease with increasing solute content. The DSC transition curves are clearly showing the effects of varying extent of partitioning of the solute between gel and fluid phases. In the C_{12}DiI case there is indication of the presence of a small, second transition at 0.05 mole fraction, which could be a result of phase separation in these mixtures. Samples showing these multiple transitions were not used in any subsequent data analysis. The range of mole fractions used in the analyses was generally 0.04 or less.

Fig. 2 shows transition enthalpies for several DSPC–C_nDiI runs as mole fraction varies between 0 and 0.05. The least-squares line through the data for each case are shown. Thus, although the uncertainties in the enthalpies are fairly large, there are definite changes in the transition enthalpy as the amount of the C_nDiI solute increase in the DSPC. The C_{12}DiI solute has a negative slope, while the others show an upward trend with increased concentration of solute.

Fig. 3 shows the data for the changes in T_m with concentration of C_nDiI in DSPC at mole fractions between 0 and 0.04. The most dramatic effect is for the C_{12}DiI solute, producing an almost 2-degree depres-

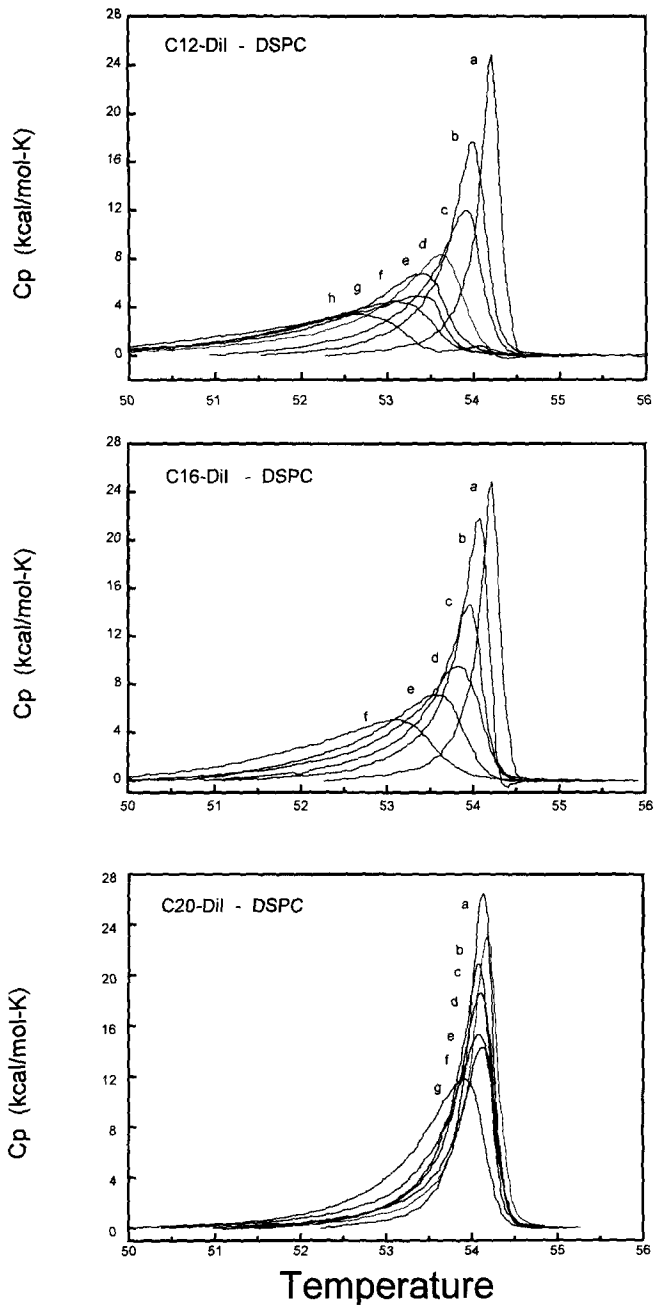

Fig. 1. Representative DSC curves for DSPC-C_nDiI mixtures. Mole fraction solutes are: C_{12}DiI: (a) 0, (b) 0.005, (c) 0.010, (d) 0.02, (e) 0.03, (f) 0.035, (g) 0.04, (h) 0.05; C_{16}DiI: (a) 0, (b) 0.005, (c) 0.01, (d) 0.02, (e) 0.03, (f) 0.04; C_{20}DiI: (a) 0, (b) 0.0046, (c) 0.0139, (d) 0.0186, (e) 0.0279, (f) 0.0371, (g) 0.0465.

sion of T_m by 5 mole percent. On the other hand, C_{20}DiI causes almost no depression of the transition temperature. The other solutes fall in between these two cases. As described in the Data Analysis section earlier, it is possible to use the treatment of Inoue et al. [19], to determine the free energy of transfer of solute between fluid and gel lipid taking into account the nonideality as an excess energy contribution to the equation for the variation of T_m with X_s. In order to

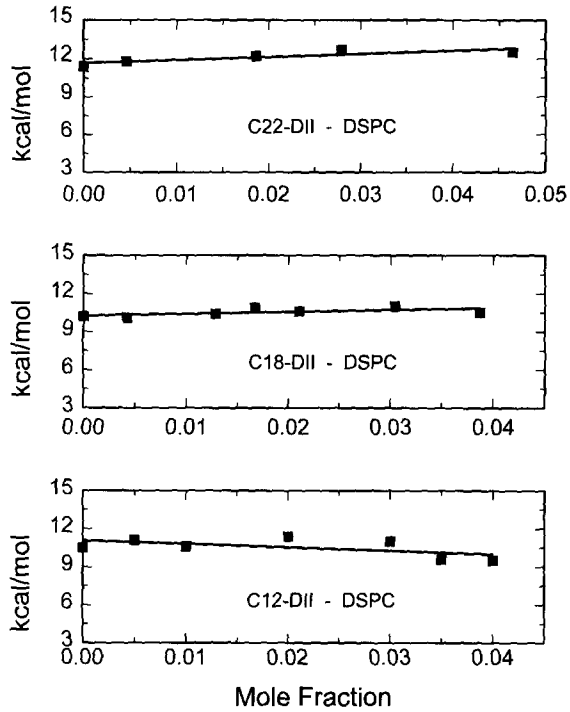

Fig. 2. Representative calorimetric enthalpy data of DSC transitions vs. mole fraction of C_nDiI for DSPC-C_nDiI mixtures. Solid lines are regression curves for the data, as described in text.

obtain the free energy, the limiting slope of the T_m vs. X_s plots is the desired quantity. (See Eqs. (1) and (2).) A nonlinear regression method gave consistent convergence on the limiting slopes for all of the cases, and the values were actually very close to values obtained from linear regression of the most dilute points in the data set. Table 1 shows the calculated net free energy of transfer, ΔG_{tr}, of the C_nDiI solutes from gel to fluid phase, $(\Delta G_s^\circ + \Delta U_s)$, and the partition coefficient, K_p, defined as the solute fluid/gel ratio. The uncertainties

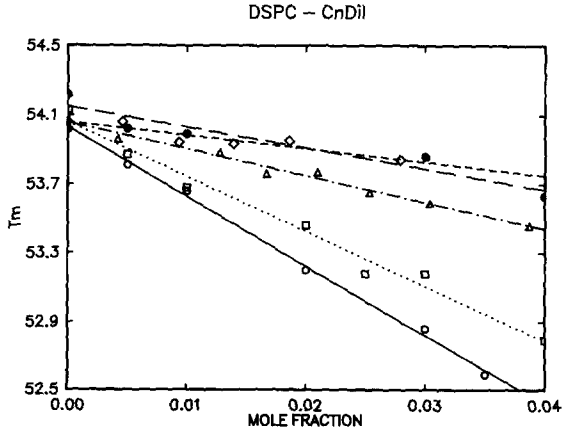

Fig. 3. Variation of T_m of gel–liquid crystal phase of transition of DSPC with mole fraction of C_nDiI solute. Curves are for C_{12}DiI (○), C_{16}DiI (□), C_{18}DiI (△), C_{20}DiI (◇) and C_{22}DiI (●).

Table 1
Thermodynamic data for fluid-gel partitioning of C_nDiI in DSPC and DPPC

Chain length	K_p	ΔG_{tr}	ΔH_{tr}	ΔH_{tr}*	ΔS_{tr}
DSPC					
C-12	6.7±0.4	−1230±40	−26±15	–	−76±40
C-16	6.4±0.5	−1200±50	3±15	0	13±40
C-18	2.1±0.1	−490±30	15± 8	19	47±20
C-20	1.3±0.1	−190±20	23± 8	26	71±20
C-22	1.5±0.1	−280±30	18±11	21	56±30
DPPC					
C-12	5.4±0.2	−1050±20	−10±11	–	−29±40
C-16	1.5±0.1	−230±50	22± 9	–	71±30
C-18	1.0±0.1	−9±50	23±12	–	127±50
C-20	1.3±0.1	−180±40	29± 7	–	93±20
C-22	2.6±0.2	−590±60	22±11	–	72±30

K_p is the partition coefficient = X_{fl}/X_{gel}. ΔG_{tr} is in cal/mol; ΔH_{tr} is in kcal/mol; ΔS_{tr} is in cal/K per mol.
* Value of ΔH is from temperature dependence of partitioning as reported in Ref. [18].

in the free energy and K_p were calculated from error estimates in the slopes of the plots.

The free energies are negative for all of the C_nDiI solutes, meaning that K_p is greater than one in each case. The solutes thus show a preference for partitioning into the fluid phase DSPC. The C_{20}DiI is closest to showing gel phase partiality, with a K_p of 1.3. These data indicate that a close match of the length of the alkyl chain in C_nDiI to the bilayer acyl chain length leads to greater partitioning into the gel phase lipid. The fact that the minimum is not obtained at equal chain lengths suggests that the head group areas are positioned slightly differently, resulting in a displacement of the solute away from the center of the bilayer. These same effects were observed for the C_nDiI solutes when using the fluorescence technique for determining K_p values in DSPC [18]. Also shown in Table 1 are estimates of the enthalpy of transfer, ΔH_{tr}, of the indocarbocyanine solutes from gel to fluid phase DSPC from the plots in Figs. 2, and using Eq. (4). To improve the slope estimates somewhat, points that fell outside the 95% confidence limits of the regression equation were eliminated, and new slopes evaluated. (This procedure eliminated no more than one point per data set, except for one, for which two points were removed.) The data in Table 1 are obtained from these refined data sets. The error estimates are obtained from the uncertainties in the slopes of the regression lines. Also shown in Table 1 are values of ΔH_{tr} obtained from the temperature dependence of K_p determined from the fluorescence quenching data [18]. The agreement is within the experimental errors of both methods. From the ΔH_{tr} and the free energy change, the entropy of transfer can be calculated at the transition temperature of the pure lipid, and these data are presented in Table 1. It is apparent from the results that within the experimental error the transfer process involves an almost complete entropy-enthalpy compensation. The free energy changes are all relatively small compared with the enthalpy effects, a condition that is typical of entropy-enthalpy compensation [23]. The consequences of these data will be discussed later.

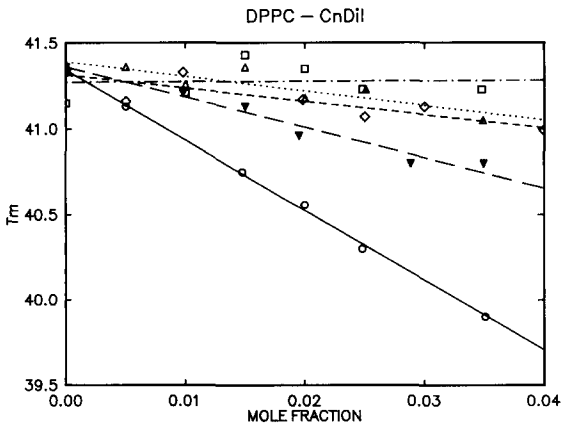

Fig. 4. Variation of T_m of gel–liquid crystal phase transition of DPPC with mole fraction of C_nDiI solute. Curves are for C_{12}DiI (○), C_{16}DiI (▼), C_{18}DiI (□), C_{20}DiI (◇) and C_{22}DiI (△).

C_nDiI-DPPC results

The DSC transition curves for DPPC-C_nDiI mixtures behave similarly to the DSPC cases. (Transition

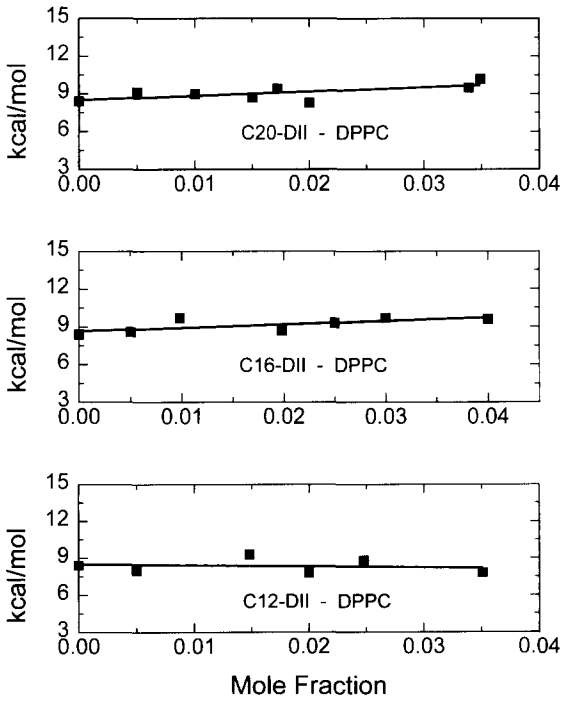

Fig. 5. Representative calorimetric enthalpy data of DSC transitions vs. mole fraction of C_nDiI for DPPC–C_nDiI mixtures. Solid lines are regression curves for the data, as described in the text.

curve data not shown in order to conserve space.) That is, there is depression of the T_m, broadening of the transitions and lowering of the $C_{p(m)}$ with increased concentration of solute in the bilayer. Fig. 4 shows the variation of T_m with mole fraction solute, and Fig. 5 the transition enthalpies for several DPPC-C_nDiI mixtures. As with DSPC, the enthalpies show a slight upward trend with increasing mole fraction of solute, except for the C_{12}DiI, which has a negative slope. These results again indicate that there is nonideality of mixing in one or both of the lipid phases. The T_m vs. X_s slopes change with alkyl chain length in the indocarbocyanines, as with DSPC. Table 1 also summarizes the calculated K_p, enthalpy and free energy of transfer values for the DPPC case. As before, there is minimum in K_p with the C_nDiI solute whose alkyl chain length approximately matches the bilayer acyl chain length. And the data also show the entropy-enthalpy compensation observed in the transfer properties in DSPC.

4. Discussion

Thermodynamic models

In a number of previous studies of the thermodynamic behavior of solutes in model membranes it was assumed that ideal solutions are formed in both phases of lipid [11,12,15]. The consequences of using the ideal vs. the regular solution approach can be examined by looking at the values of K_p calculated from the data sets by the two methods. Table 2 shows the K_p values obtained from the results of C_nDiI partitioning in DPPC and DSPC calculated according to the regular and ideal solution models. The ideal model uses the equations of Sturtevant [12] for determining K_p from DSC data. It is notable that in the DPPC model membrane the differences between the two methods is relatively small except for the C_{12}DiI case, where chain mismatch is greatest between the solute and the bilayer. On the other hand, there are significant differences between the two sets of numbers for the DSPC lipid phases. The closest agreement is for the C_{18}- and C_{20}-solutes in DSPC, where the lengths of the alkyl chains in the DiI's are similar to the bilayer thickness. The K_p data indicate that the greater effect the solute has on the T_m values (the steeper the slope of the T_m vs. X_s line), the greater the deviations between the ideal and regular solution calculations. A steeper negative slope implies that in one or the other of the two lipid phases there is significant interaction, either a stabilizing effect in the fluid phase, or a destabilizing interaction in the gel phase. Assuming that the fluid phase is more likely to behave ideally than the gel phase, which has been observed for some phase diagrams of lipid mixtures [20–22], an explanation for the steeper slopes and larger deviations from ideal behavior is that there is significant destabilization of the solute in the gel phase. Chain mismatch of 4–6 carbon atoms could cause significant disruption of packing in the gel phase in the vicinity of the solute. The breakdown of interactions between chains in the gel would lead to a favorable enthalpy of transfer to fluid phase. As chain lengths of the solutes become closer to the bilayer thickness, less disruption occurs and the interactions are less overall favorable to the fluid phase. The disruptions in the gel phase in the extreme cases of mismatch of bilayer thickness with solute alkyl chains thus can explain why the agreement between the ideal and regular solution models breaks down for those cases.

These ideas regarding chain mismatch are supported by studies of phase diagrams of mixtures of phosphatidylcholines reported by Mabrey and Sturtevant [20]. It was found that dimyristoyl-PC (DMPC) and DPPC formed simple phase diagrams that were slightly nonideal. On the other hand, mixtures of dilauryl-PC and DSPC, where the acyl-chain mismatch is 6 carbons, there was extreme nonideality that leads to monotectic behavior in the phase diagram. Beyond about 15 mole percent DLPC there is phase separation in these mixtures [20]. Mason has published similar results with a series of mixtures of DSPC with stearoyl-PC's in which the SN-2 carbon atom is substituted with C_{10}- to C_{16}-acyl chains [21]. The case with a C_{16}-chain in the SN-2 position shows slight deviations from ideal behavior with DSPC, while the C_{10}- and C_{12}-homologs exhibit complex phase diagrams in which phase separation definitely occurs at higher concentrations of the shorter chain component. All of these studies point to the sensitivity of phase behavior to acyl chain matching when mixtures of lipids are formed in a bilayer structure.

Table 2
Comparison of K_p using ideal or regular solution model for partitioning of C_nDiI in DSPC and DPPC

Chain length	K_p (ideal)	K_p (regular)
DSPC		
C-12	37.0	6.7
C-16	13.7	6.4
C-18	2.2	2.1
C-20	1.3	1.3
C-22	1.5	1.5
DPPC		
C-12	11.5	5.4
C-16	1.5	1.5
C-18	1.0	1.0
C-20	1.3	1.3
C-22	2.8	2.6

C_nDiI partitioning comparisons

The values of K_p obtained from the DSC experiments provide an internally consistent way to compare partitioning behavior of the C_nDiI solutes. The DPPC and DSPC results indicate several trends, as shown in Fig. 6. Clearly, the length of the alkyl chains in the probes relative to bilayer thickness is one important factor in determining the values of K_p, as mentioned above. The short chain C_{12}DiI shows high preference for the fluid phase with K_p values of about 6.0 for both DPPC and DSPC. The trend in the values of K_p is that as the alkyl chain length increases, K_p gets smaller; that is, less fluid phase partitioning occurs. In the DPPC gel-fluid mixture when the alkyl chain length is C_{18}- in the probe, $K_p = 1.0$, and is a minimum, but then as C_n- increases further, the partition coefficient increases again. Similar trends are seen in the DSPC results, except that the minimum K_p occurs at the C_{20}-solute. These minima occur in both cases when the alkyl chain length is about two carbons longer than the acyl chain length of the bilayer lipid. The fact that an exact match of alkyl and acyl chains does not occur at the minimum K_p is likely a result of the differences in the structure of the headgroup of the lipid, compared with the indocarbocyanine group. (This argument presumes that the alkyl and acyl chains are in parallel conformations within the bilayer.)

Examination of the enthalpies of transfer of the C_nDiI solutes between gel and fluid phase shows that K_p is determined by a balance of enthalpy and entropy effects. The trends are shown in Fig. 7. While the transfer enthalpies determined from the DSC curves have relatively high uncertainties, there are statistically significant slopes for most of the curves in Figs. 2 and 5. As with the K_p values (and thus the free energies),

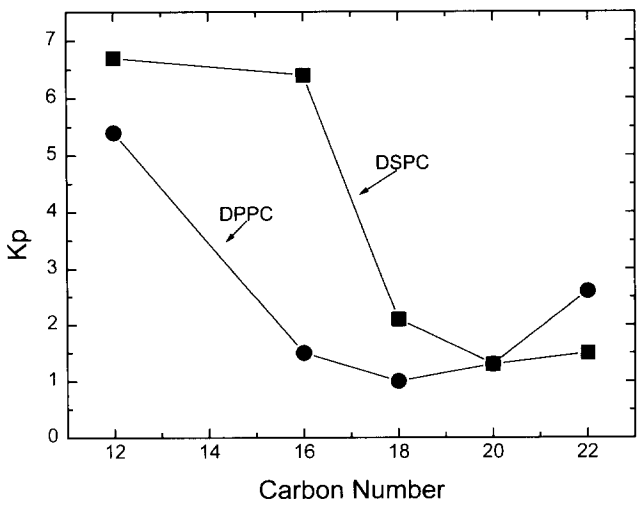

Fig. 6. Variation of the partition coefficient, K_p, with carbon number of the alkyl chains in the C_nDiI solutes for DSPC and DPPC bilayers.

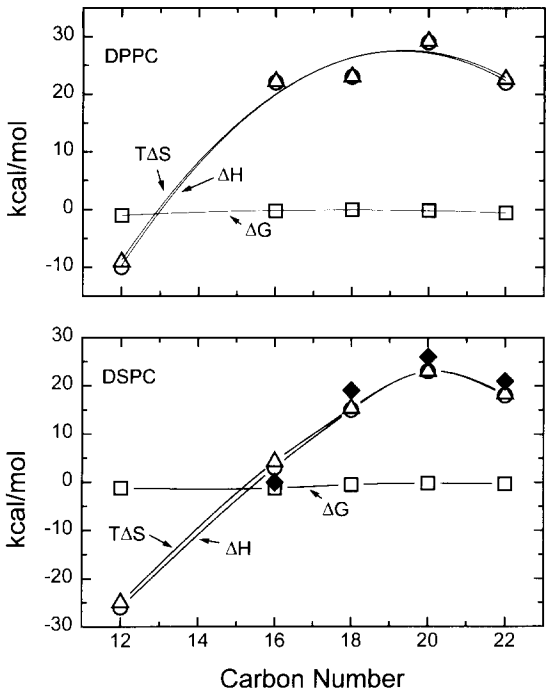

Fig. 7. Variation of thermodynamic properties of transfer of solutes, C_nDiI, where n is the carbon number in the alkyl chains, from gel to fluid phase DSPC and DPPC bilayers. Free energy (□), enthalpy (○) and TΔS (△) are shown for each lipid bilayer. The solid diamonds (♦) in the DSPC graph are enthalpy of transfer data taken from Ref. [18], based on fluorescence measurements.

there are trends in the enthalpies with variation in chain length, as shown in Fig. 7. For both DPPC and DSPC bilayers the transfer enthalpy starts out negative at the C_{12}DiI solute and then increases to a positive maximum near the 20-carbon analog. The trend that the enthalpy of transfer increases from quite negative values to positive supports the argument presented above that chain mismatch in the gel phase would raise the enthalpy of the gel phase, thus leading to a net negative transfer enthalpy. On the other hand, when the chains are nearly matched, so that interactions between solute and bilayer lipid are optimized, the enthalpy is lowered in the gel phase, and a positive transfer enthalpy occurs. The enthalpy-entropy compensation makes sense under this scenario. Also shown in Fig. 7 are enthalpy of transfer values for several of the C_nDiI solutes obtained from the temperature dependence of partition coefficients determined by the fluorescence quenching technique [18]. The agreement is quite good considering the uncertainties in the measurements.

It is significant that, as determined by DSC, none of the indocarbocyanine solutes shows an actual preference for the gel phase lipid ($K_p < 1$). This result is in contrast to the values of K_p determined from the fluorescence quenching method for which all of the K_p values are less than one for the DPPC gel phase when

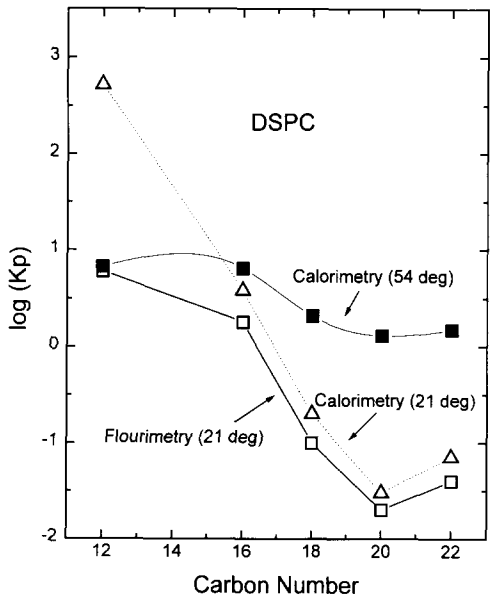

Fig. 8. Plots of log K_p, the partition coefficient for C_nDiI solutes, vs. the number of carbon atoms in the alkyl chain of the solute in DSPC. Shown are the data determined by fluorescence quenching (Ref. [18]) at 21°C, and data obtained at 54°C by DSC measurements. Also shown are the data from DSC measurements that have been corrected to 21°C using the van't Hoff relation, and the calorimetric enthalpies for the DSPC transitions.

in equilibrium with (7,6)PC fluid phase [18]. For the DSPC gel phase mixed with (7,6)PC, the C_{12}- and C_{16}-solutes have K_p values greater than 1, while the longer chain probes have partition coefficients below 0.1. Fig. 8 shows a comparison of the partition coefficients (on a log scale for plotting convenience) for the C_nDiI solutes in DSPC determined by the DSC and fluorescence methods. The figure shows that there are differences between the values obtained by DSC and by fluorescence quenching. However, the differences arise as a consequence of the experimental details of the two methods used in the evaluation K_p. The fluorescence measurements are obtained from a direct measure of the amount of residual fluorescence in the gel phase as the mole fraction of quenching, fluid phase is increased. The partitioning equilibrium in this circumstance is attained at 21°C. The DSC measurements, on the other hand, are made at the T_m of the gel-fluid phase transition, about 40° for DPPC and 53° for DSPC. Thus, there is about a 20 to 30 degree difference in temperature of measurement for the two methods. One can use the van't Hoff relation:

$$\ln\left(\frac{K_2}{K_1}\right) = -\frac{\Delta H_o}{R}\left[\frac{1}{T_2} - \frac{1}{T_1}\right] \quad (5)$$

to calculate the partition coefficient from one temperature to the value at another, and Fig. 8 shows a comparison of the values of K_p obtained from the DSC data at T_m in each case, corrected to 21° from the enthalpies of transfer determined by DSC and given in Table 1. Except for the C_{12}DiI case, the agreement is quite good, particularly considering the rather different methodology used to obtain values of the partition coefficients.

5. Conclusions

The results presented here suggest that application of the regular solution treatment to DSC transition data can provide a useful way to examine lipid–lipid interactions.

Comparison of the resulting thermodynamic parameters shows specific trends in the behavior of the solutes in bilayer membranes. By systematic measurement of the transfer thermodynamics it should be possible to determine trends in the effects of structure on the interactions within the bilayer environment. We are in the process of examining various lipid combinations with this purpose in mind, and using the techniques described here.

6. Acknowledgments

This work was supported by a grant from the National Science Foundation (Grant No. DMB 8820849). The authors appreciate the technical assistance of Mr. Edwin Mereand, and the useful discussions with Dr. Gerald Feigenson of Cornell University.

7. References

[1] Yguerabide, J. and Foster, M.C. (1979) J. Membr. Biol. 45, 109–123.
[2] Lentz, B.E., Barenholtz, Y. and Thompson, T.E. (1976) Biochemistry 15, 4529–4537.
[3] Sklar, L.A., Miljanich, G.P. and Dratz, E.A. (1979) Biochemistry 18, 1707–1716.
[4] London, E. and Feigenson, G.W. (1981) Biochim. Biophys. Acta 649, 89–97.
[5] Welti, R. and Silbert, D.F. (1982) Biochemistry 21, 5685–5689.
[6] Florine, K.I. and Feigenson, G.W. (1987) Biochemistry 26, 1757–1768.
[7] Huang, N., Florine-Casteel, K.I., Feigenson, G.W. and Spink, C.H. (1988) Biochim. Biophys. Acta 939, 124–130.
[8] London, E. and Feigenson, G.W. (1981) Biochemistry 20, 1932–1938.
[9] Florine, K.I. and Feigenson, G.W. (1987) Biochemistry 26, 2978–2983.
[10] Hauser, H. and Shipley, G.G. (1984) Biochemistry 23, 34–41.
[11] Sturtevant, J.M. (1982) Proc. Natl. Acad. Sci. USA 79, 3963–3967.
[12] Sturtevant, J.M. (1984) Proc. Natl. Acad. Sci. USA 81, 1398–1400.
[13] Klauser, R.D. and Wolf, D.E. (1980) Biochemistry 19, 6199–6203.
[14] Ethier, M.F., Wolf, D.E. and Melchior, D.L. (1983) Biochemistry 22, 1178–1182.

[15] Fumero, J. Bammel, B.P. Hopkins, H.P. and Smith, J.C. (1988) Biochim. Biophys. Acta 944, 164–176.
[16] Derzko, Z. and Jacobson, K. (1980) Biochemistry 19, 6050–6057.
[17] Aranda, F.J. and Gomez-Fernandez, J.C. (1982) Arch. Biochem. Biophys. 218, 525–530.
[18] Spink, C.H., Yeager, M.D. and Feigenson, G.W. (1990) Biochim. Biophys. Acta 1023, 25–33.
[19] Inoue, T., Suezaki, Y., Fukushima, K. and Shimozawa, R. (1990) Chem. Phys. Lipids 55, 145–154.
[20] Mabrey, S. and Sturtevant, J.M. (1976) Proc. Natl. Acad. Sci. USA 73, 3862–3866.
[21] Mason, J.T. (1988) Biochemistry 27, 4421–4429.
[22] Lee, A.G. (1977) Biochim. Biophys. Acta 472, 285–344.
[23] Tanford, C. (1973) The Hydrophobic Effect, Wiley, New York.